Preprint 12th SiliconPV Conference, 27-30 March, 2022, Konstanz

Various Impacts of Firing Temperature on Crystalline Silicon

Christian Fischer[a)], Annika Zuschlag[b)] and Giso Hahn[c)]

Department of Physics, University of Konstanz, 78457 Konstanz, Germany

[a)] *Corresponding author: christian.fischer@uni-konstanz.de*
[b)]*annika.zuschlag@uni-konstanz.de*
[c)]*giso.hahn@uni-konstanz.de*

Abstract. The firing step in the manufacturing process of a solar cell is decisive for various parameters. For example, hydrogen from the passivation layers is introduced to the interfaces and into the sample. This serves to passivate defects and thus leads to an increase in the lifetime of the charge carriers. Conversely, higher firing temperatures result in stronger light- and elevated temperature-induced degradation (LeTID) and can introduce more impurities. In addition, contact formation occurs during firing. Therefore, the ideal firing temperature is a difficult to find optimum with various dependencies. In this work, we varied firing peak set temperatures between 650°C and 950°C. In dependence of the firing temperature, we studied the initial lifetime and iron concentration in float zone (FZ) and Czochralski (Cz) grown silicon wafers with and without phosphorus gettering and with aluminum oxide (AlO_x) and hydrogen-rich silicon nitride (SiN_x:H) passivation. With atomic layer deposited (ALD) AlO_x passivation the initial lifetime is decreasing with higher firing temperatures, and interstitial iron concentration ([Fe_i]) is rising to a saturation in the range of 10^{11} cm^{-3} at around 800°C. In contrast, SiN_x:H passivation results in highest lifetimes at around 800°C. Regarding LeTID, the results for SiN_x:H passivated samples are in good agreement to literature and an increase in maximum degradation is observed with higher firing temperatures. However, with low hydrogen-containing ALD AlO_x it is more complicated. For Cz material with ALD AlO_x no clear correlation between firing temperature and extent of degradation could be found. Therefore, finding an optimum firing temperature remains a challenge for each material and passivation-layer-stack.

INTRODUCTION

The firing step is a simple but crucial step in the manufacturing process of a solar cell. Depending on material and passivation layer stacks, an ideal firing temperature has to be found.

The firing temperature is decisive for the initial lifetime of samples, as it impacts the activation and deactivation of defects and possible introduction of impurities, e. g. iron. It influences the hydrogenation of the solar cell, because during this short high temperature step hydrogen is released from passivating layers like SiN_x:H [1]. Hydrogen diffusing into the silicon can passivate defects within the material and at interfaces [2]. In this way, firing temperature additionally contributes indirectly via the hydrogen release to the material quality of the solar cell. On the other hand, it is well known, that also detrimental effects like light and elevated temperature induced degradation (LeTID) are triggered by the firing step [3, 4]. Finally firing temperature is essential for contact formation [5] and therefore an optimization is a quite sophisticated challenge.

In this work, we investigate Cz and FZ wafers with lower hydrogen and hydrogen-rich passivation layers with respect to the firing temperature. We determine the change of iron contamination in the silicon bulk, the impact on charge carrier lifetime and the degradation behavior.

EXPERIMENTAL

In this experiment FZ (~2.1 Ωcm) and Cz (~1.7 Ωcm) wafers are used. Both materials are boron-doped and diamond wire-sawn. Wafers were laser cut to 5x5 cm^2 samples. A process flow diagram is given in Fig. 1.

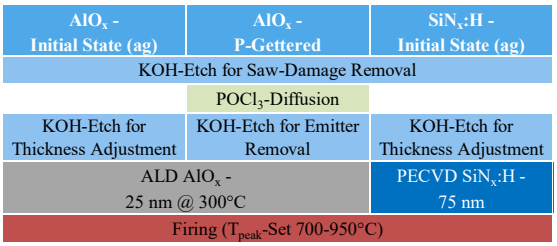

FIGURE 1. Process flow diagram of sample preparation with etching and passivation steps.

After saw damage removal with KOH and subsequent cleaning one group of the samples received a phosphorus diffusion (~50 Ω/□). The deposited phosphorus silicate glass (PSG) serves as getter sink especially for metal impurities, including iron [6]. Subsequently, PSG and emitter were removed. During the etching steps, care was taken to ensure that the same final sample thickness was achieved on P-gettered and ungettered (ag) samples. For this purpose, about 20 µm per side in total were removed from all samples.

For passivation, one group was coated on both sides with an AlO_x layer of about 25 nm thickness at 300°C from an atomic layer deposition (ALD) system from Oxford Instruments (FlexAL-Reactor). The other group received a (75 ± 5) nm thick SiN_x:H layer by direct plasma-enhanced chemical vapor deposition (PECVD) at 450°C in a tool from centrotherm. The passivated samples were fired in a belt furnace using a stand-off. The peak set temperature was varied between 700°C and 950°C. To measure sample temperature, a thermocouple connected to the sample during firing was used.

Photoconductance decay (PCD) measurements for injection-dependent lifetime and photoluminescence (PL) measurements to check homogeneity were performed to characterize the initial state of samples. Interstitial iron concentration was determined by PCD measurements of the samples in associated (FeB) and dissociated (Fe_i) state according to Zoth and Bergholz [7] and Macdonald et al. [8]. The (FeB) state was achieved by storage in the dark at room temperature for at least 24 h. Dissociation was forced by illumination with about 2 sun equivalent light for at least 45 s. Selected ungettered samples were re-passivated after firing with iodine-ethanol. The iodine-ethanol passivation was performed as described by Sopori et al. [9]. In addition, selected samples were treated at ~1 sun and 130°C and lifetime was measured in-situ on a WCT-120TS from Sinton Instruments (T-PCD). Based on these lifetimes obtained by T-PCD, a lifetime-equivalent defect density [10] at an injection corresponding to $^1/_{10}$ N_D was calculated.

RESULTS

In the following, sample firing temperature is the actual temperature measured on a wafer during the belt firing process. This temperature results from belt furnace parameters like belt speed and set temperatures and from material characteristics like thickness, optical properties and doping of the wafer. Most critical are the peak firing temperature and the cooling ramps. In this experiment we kept cooling ramps constant and only varied peak temperature. Therefore, we first consider the relationship of firing peak set temperature and sample peak temperature (see Fig. 2).

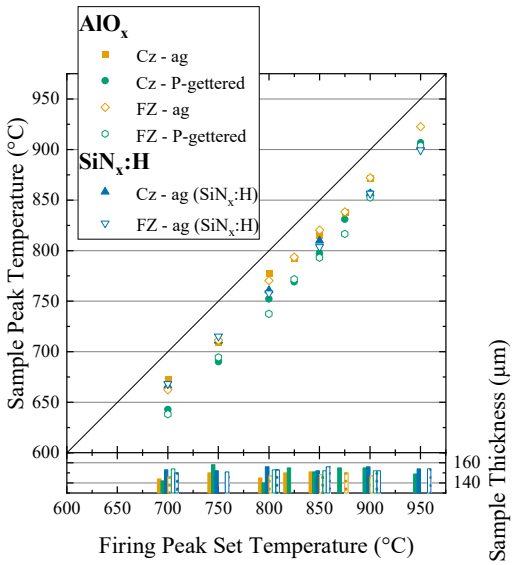

FIGURE 2. Measured sample peak temperature is given with peak set temperature and sample thickness.

Different passivation layers (AlO_x and SiN_x:H) with their differing optical properties influence sample peak temperature. SiN_x:H sample peak temperature is increasing slightly slower with peak set temperature than that of AlO_x passivated samples. Between the materials FZ and Cz no significant difference can be found regarding the resulting sample peak temperature. This is probably due to similar properties as both materials are diamond wire-sawn and etched to comparable thicknesses. However, there is a difference of approx. 20°C between AlO_x samples in the initial state and P-gettered samples. A correlation with sample thickness can be ruled out as slight variations in thickness do not correspond to temperature variations (see Fig. 2). Therefore, we conclude, the cause is probably due to slightly changed optical properties as reflectance measurements indicate (see Fig. 3). This could be a result of changed etching behavior for the P-gettered samples, which may affect the light coupling and thus the temperature of the samples.

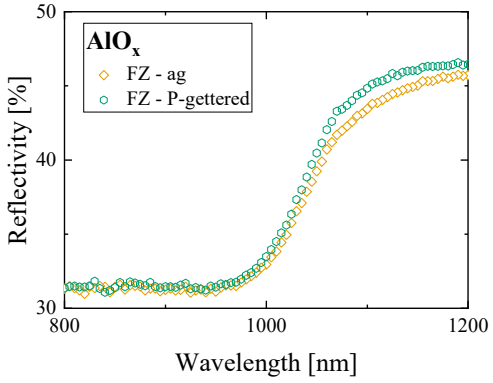

FIGURE 3. Measured reflectivity of AlO_x passivated FZ samples after firing.

PL images show a homogeneous passivation for all samples with small scratches due to the thermocouple. Lifetime in Fe_i state and interstitial iron concentrations shown in Fig. 4 were determined in each case at the injection corresponding to one tenth of the doping (N_D) of the respective materials.

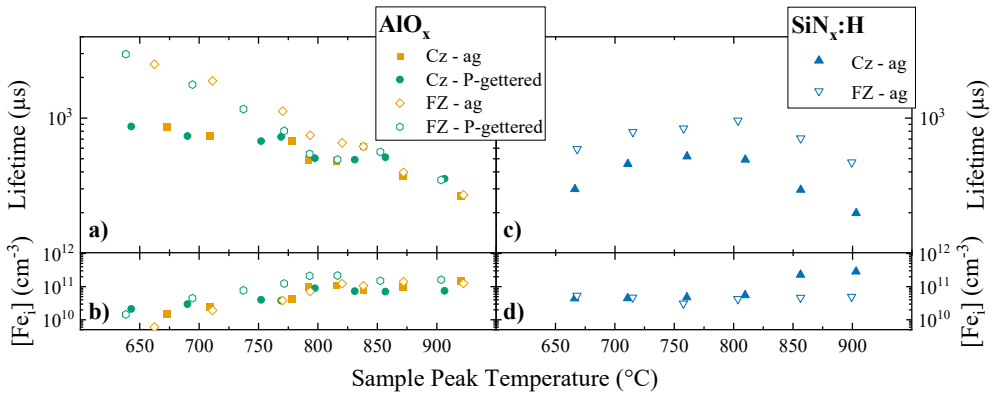

FIGURE 4. a) Lifetimes from PCD measurement of AlO_x passivated samples in (Fe_i) state at injection corresponding to $^1/_{10}$ N_D.
b) Interstitial iron concentration of AlO_x passivated samples.
c) Lifetimes from PCD measurements of SiN_x:H passivated samples in (Fe_i) state at injection corresponding to $^1/_{10}$ N_D.
d) Interstitial iron concentration of SiN_x:H passivated samples.

For AlO_x passivated samples, the lifetimes of the FZ samples at low firing temperatures are significantly higher than those of the Cz material (Fig. 4a). This results from higher bulk material quality of FZ wafers. The difference decreases with increasing firing temperature and is virtually non-existent for firing temperatures above 850°C. It should be noted that for both materials the lifetimes decrease with increasing peak sample temperature during firing. The cause of this decrease is partially due to an increasing iron concentration in the silicon bulk. Almost no difference in lifetime or iron concentration could be achieved by the phosphorus diffusion (P-gettering). This could indicate that iron was introduced after gettering. Apart from degradation of material quality, a reduced surface passivation is a further possibility to explain the reduced lifetimes in all samples. With iodine ethanol re-passivation (data given in Tab. I) it could be shown that there is a strong detrimental effect of the increased firing temperature to the bulk for FZ, as lifetimes are not increasing after re-passivation (the slightly increased lifetime after re-passivation for Cz fired at 900°C is not yet understood). Therefore, we conclude that the iron was introduced into the silicon samples during sample processing, and probably during the firing step itself.

TABLE 1. Lifetime values before and after iodine ethanol re-passivation ($\Delta n = {}^1/_{10}$ N_D).

Peak firing temperature	700°C	800°C	900°C
Cz – AlO_x passivation	708 µs	410 µs	196 µs
Cz – Iodine ethanol re-passivation	421 µs	244 µs	267 µs
FZ – AlO_x passivation	3208 µs	837 µs	227 µs
FZ – Iodine ethanol re-passivation	661 µs	353 µs	162 µs

This is also in good agreement with the results obtained by SiN_x:H passivated samples (Fig. 4 c), d)). These samples show a constant level of iron contamination similar to the level determined in low temperature fired AlO_x samples. A possible explanation is that SiN_x:H serves as a diffusion barrier for iron impurities and therefore no more iron is introduced. Another option is that SiN_x:H serves as a getter-sink for iron like proposed in literature [11]. The stepwise increase of [Fe_i] in Cz above 850°C could be caused by dissolving iron clusters in the material, although such high amounts of iron are not expected from Cz crystal growth.

Lifetimes for low firing temperatures of SiN_x:H samples are inferior to AlO_x passivated ones. This changes with higher firing temperatures as this triggers additional hydrogen release [1], and this is beneficial for τ_{eff}. Highest lifetimes are achieved with sample peak firing temperatures between 750°C and 800°C. With higher firing temperatures probably detrimental effects of temperature are exceeding beneficial effects of hydrogen passivation of defects.

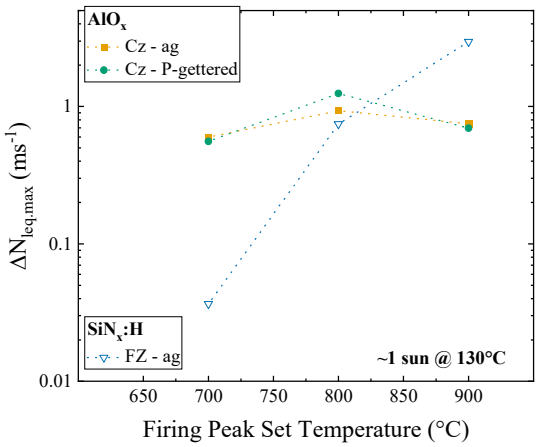

FIGURE 5. Maximum lifetime-equivalent defect density $N_{leq,max}$ determined by automated lifetime measurements during treatment at ~1 sun and 130°C after firing.

Regarding the extent of degradation shown in Fig. 5, hydrogen-rich SiN_x:H passivated FZ samples show the expected behavior of an increase in $N_{leq,max}$ with the firing temperature [12]. However, AlO_x passivated wafers behave differently. Comparison are only possible qualitatively, as Cz and FZ samples differ significantly in degradation extent. Maximum degradation is observed in Cz wafers fired at 800°C. This could possibly be attributed to an overlap of boron-oxygen related light induced degradation (BO-LID), LeTID and subsequent regeneration. In addition, ALD AlO_x has quite low hydrogen and therefore hydrogenation of the samples is reduced.

CONCLUSION

The firing temperature is a crucial factor in solar cell and lifetime sample fabrication. Measurement of actual sample peak temperature is essential, since sample temperature can deviate significantly from the set temperature. We could show that especially optical properties like reflectance can influence heat absorption and thus sample peak firing temperature. Depending on the passivation layers different correlations between initial lifetime and firing temperature were found. The less hydrogen containing AlO_x layers showed the best performance at lower firing temperatures. Hydrogen-rich SiN_x:H requires a certain minimum firing temperature (750-800°C) for good initial effective lifetimes. With higher temperature lifetime is decreasing again.

As activation, deactivation and introduction of impurities can also be attributed to the firing process, we exemplarily investigated interstitial iron concentration in dependence of firing temperature. [Fe_i] remains on a quite constant level with SiN_x:H passivation independent of firing temperature, expect of Cz samples fired above 850°C. However, AlO_x passivated samples show an increase in [Fe_i] with firing temperature. This could possibly indicate that iron impurities are introduced through the thin AlO_x layer during the firing process, whereas SiN_x:H presents a sufficient diffusion barrier or gettering layer.

Furthermore, degradation phenomena like BO-LID or LeTID are influenced by the firing temperature. LeTID is generally low at low firing temperatures and increasing with higher temperatures. However, as it is dependent on hydrogen, this behavior could only be observed on SiN_x:H passivated hydrogen-rich samples.

While firing temperature is also critical for solar cell contact formation and therefore additionally restricted, finding an optimum firing temperature is a sophisticated challenge.

ACKNOWLEDGMENTS

Part of this work was supported by the German BMWK under contract 0324204B. The content of the publication is the responsibility of the authors. The authors would like to thank D. Skorka, L. Mahlstaedt, and L. Dobler for technical support and assistance with experiments.

REFERENCES

1. B. Sopori, Y. Zhang, R. Reedy, K. Jones, Y. Yan, M. Al-Jassim, B. Bathey, J. Kalejs, "A comprehensive model of hydrogen transport into a solar cell during silicon nitride processing for fire-through metallization", in *Proc. 31st IEEE Photovoltaic Specialists Conference-2005,* pp. 1039-1042.
2. R. Rizk, P. de Mierry, D. Ballutaud, M. Aucouturier, D. Mathiot, Phys. Rev. B **44**, 6141-6151 (1991).
3. R. Eberle, W. Kwapil, F. Schindler, M. C. Schubert, S. W. Glunz, Phys. Status Solidi RRL **10**, 861-865 (2016).
4. M. Kim, S. Wenham, V. Unsur, A. Ebong, B. Hallam, "Impact of Rapid Firing Thermal Processes on Meta-Stable Defects: Preformation of the LeTID and the Suppression of B-O Defects", in *7th World Conference on Photovoltaic Energy Conversion-2018*, pp. 0341-0346.
5. M. M. Hilali, M. M. Al-Jassim, B. To, H. Moutinho, A. Rohatgi, S. Asher, J. Electrochem. Soc. 152, G742 (2005).
6. S. A. McHugo, H. Hieslmair, E. R. Weber, Appl. Phys. **64**, 127-137 (1997).
7. G. Zoth and W. Bergholz, J. Appl. Phys. **67**, 6764-6771 (1990).
8. D. H. Macdonald, L. J. Geerligs, A. Azzizi, J. Appl. Phys. **95**, 1021-1028 (2004).
9. B. Sopori, P. Rupnowski, J. Appel, V. Mehta, C. Li, S. Johnston, "Wafer preparation and iodine/ethanol passivation procedure for reproducible minority-carrier lifetime assessment", in *Proc. 33rd IEEE Photovoltaic Specialists Conference-2008*, pp. 1364-1367.
10. A. Herguth, IEEE J. Photovolt. **9**, 1182-1194 (2019).
11. Y. Liu, C. Sun, V. P. Markevich, A. R. Peaker, J. D. Murphy, D. Macdonald, J. Appl. Phys. **120**, 193103 (2016).
12. D. Chen, M. V. Contreras, A. Ciesla, P. Hamer, B. Hallam, M. Abbott, C. Chan, Prog. Photovolt.: Res. Appl. **29**(11), 1180-1201 (2021).